lncRNA RPPH1 promotes non-small cell lung cancer progression through the miR-326/WNT2B axis

YUYING WU, KEWEI CHENG, WENJUN LIANG and XIAOHUA WANG

Department of Respiratory and Critical Care Medicine, The Affiliated Changzhou No. 2 People's Hospital of Nanjing Medical University, Changzhou, Jiangsu 213000, P.R. China

Received September 16, 2019; Accepted June 12, 2020

DOI: 10.3892/ol.2020.11966

Abstract. Long non-coding RNAs (lncRNAs) serve important regulatory roles in human tumors. The aim of the present study was to examine the role of ribonuclease P RNA component H1 (RPPH1) in non-small cell lung cancer (NSCLC). RPPH1 expression was assessed in datasets from The Cancer Genome Atlas, as well as lung cancer cell lines and patients with NSCLC. RPPH1 was significantly upregulated in NSCLC cell lines, compared with a normal lung epithelial cell line. Moreover, high RPPH1 expression was associated with poor overall survival and disease progression. RPPH1 was knocked down in A549 and H1299 cells using short hairpin (sh) RNA constructs, and the expressions of target genes and proteins were determined by reverse transcription-quantitative PCR and western blotting. Cell invasion potential was also determined using Transwell Matrigel assays. Compared with the negative control, RPPH1 silencing significantly reduced the number of invading cells, increased E-cadherin expression and reduced vimentin protein expression. Cell resistance to cisplatin/cis-diamminedichloridoplatinum (CDDP) was also evaluated using Cell Counting Kit-8 and colony formation assays. RPPH1 overexpression increased the resistance of A549 and H1299 cells to CDDP. Moreover, the potential interactions between RPPH1, microRNA (miR)-326 and Wnt family member 2B (WNT2B) were investigated using luciferase reporter assays and co-transfection experiments. MiR-326 expression was directly inhibited by RPPH1. In A549 cells co-transfected with shRPPH1 and miR-326 inhibitor, the invading cell number significantly increased compared with cells transfected with shRPPH1 alone. In addition, E-cadherin expression levels were reduced, and vimentin was upregulated. MiR-326 overexpression partially reduced the resistance of A549 cells to CDDP induced by RPPH1 overexpression. WNT2B expression was directly suppressed using miR-326. A549 cells co-transfected with a miR-326 mimic and a WNT2B overexpression vector demonstrated increased invasion potential, reduced E-cadherin and increased vimentin protein expression levels, compared with cells transfected with the mimic alone. miR-326 overexpression reduced CDDP resistance in A549 cells. However, co-transfection with WNT2B partially enhanced CDDP resistance, compared with the mimic alone. In conclusion, RPPH1 promoted NSCLC progression and lung cancer cell resistance to CDDP through miR-326 and WNT2B.

Introduction

Non-small-cell lung cancer (NSCLC) is one of the most lethal types of cancer worldwide, accounting for 85% of lung cancer cases (1). The majority of patients with NSCLC die within one year of diagnosis and the 5-year survival rate is as low as 17.8% (2). Surgical resection combined with postoperative adjuvant therapies, such as chemotherapy and radiotherapy, is a common treatment for NSCLC (3). The inability to diagnose and treat the condition in the early stages is an important factor underlying the low survival rate of patients with NSCLC (4). Thus, understanding the molecular mechanisms of NSCLC onset and progression would provide invaluable insight into early diagnosis and treatment, thereby enabling effective targeted therapy.

In recent years, dysregulation of long non-coding RNAs (lncRNAs) has been demonstrated to be an important causative factor behind the development of NSCLC. Several lncRNAs, such as actin filament associated protein 1 antisense RNA, X-inactive specific transcript and maternally expressed 3, have been implicated in NSCLC progression (5-7) and may represent potential effective targets for diagnosis and targeted therapy for NSCLC. Ribonuclease P RNA component H1 (RPPH1), a novel lncRNA, serves a role in the pathogenesis of several human diseases. For instance, a previous study suggested that RPPH1 could promote hippocampal neuron dendritic spine formation by regulating microRNA (miR)-330-5p and cell division cycle 42 in Alzheimer's disease (8). RPPH1 is also thought to be involved in the inflammatory pathogenesis of diabetic nephropathy. Indeed, in a mouse model of diabetic nephropathy, RPPH1 was abnormally overexpressed in renal

Correspondence to: Dr Xiaohua Wang, Department of Respiratory and Critical Care Medicine, The Affiliated Changzhou No. 2 People's Hospital of Nanjing Medical University, 29 Xinglongxiang Street, Changzhou, Jiangsu 213000, P.R. China
E-mail: xiaohuawang76@126.com

Key words: non-small cell lung cancer, progression, ribonuclease P RNA component H1, microRNA-326, Wnt family member 2B

tissue and enhanced the release of inflammatory cytokines, including tumor necrosis factor-α and monocyte chemotactic protein-1 (9). Moreover, Zhang *et al* (10) demonstrated that RPPH1 upregulation enhanced the proliferative and colony formation abilities of breast cancer cells. It has also been suggested that RPPH1 may aggravate the development of breast cancer by suppressing the expression of miR-122 (10). Liang *et al* (10) demonstrated that RPPH1 could promote colorectal cancer metastasis by interacting with tubulin β3 class III and promoting exosome-mediated macrophage M2 polarization. Furthermore, Lei *et al* (11) suggested that RPPH1 could enhance human acute myeloid leukemia cell proliferation, migration and invasion by reducing the expression of miR-330-5p (11).

Although evidence suggested that RPPH1 may be associated with the onset of several diseases, the exact function and mechanism of action underlying the role of RPPH1 in human disease remain unclear. In the present study, the role of RPPH1 in NSCLC progression was evaluated by studying its interaction with miR-326 and Wnt family member 2B (WNT2B). miR-326 has been previously implicated in the development of several types of human tumors, including cervical cancer, lung cancer and breast cancer (12-14). WNT2B is a crucial protein in the Wnt signaling pathway that can act as an oncogene (15,16). These findings may provide a novel molecular target and a theoretical basis for the targeted therapy of NSCLC.

Materials and methods

The Cancer Genome Atlas (TCGA) analysis. RPPH1 expression data in tumor (n=180) and adjacent normal tissues (n=171) from patients with NSCLC were downloaded from TCGA (https://tcga-data.nci.nih.gov/tcga/). The effect of RPPH1 expression levels on patient 80-month overall survival of patients was also evaluated using Kaplan-Meier survival analysis. Lastly, the effect of RRPH1 expression on clinical stages was also assessed (17).

Cell lines and culture. The human BEAS-2B normal lung epithelial cell line, as well as H358, A549, H1299 and H1650 NSCLC cell lines were purchased from The Cell Bank of Type Culture Collection of the Chinese Academy of Sciences. All cell lines were separately maintained in complete DMEM (Thermo Fisher Scientific, Inc.) supplemented with 10% FBS (Thermo Fisher Scientific, Inc.) at 37˚C with 5% CO_2.

Reverse transcription-quantitative PCR (RT-qPCR). BEAS-2B, H358, A549, H1299 and H1650 cells were trypsinized, then collected for total RNA extraction using TRIzol® reagent (Invitrogen; Thermo Fisher Scientific, Inc.). Reverse transcription was performed in 20-μl reactions using the Prime Script™ RT reagent kit (Takara Bio, Inc.) at 37˚C for 15 min. The resulting cDNA templates were used for RT-qPCR, which was performed using the SYBR-Green PCR Master Mix kit (Takara Bio, Inc.) on the ABI Prism 7300 Sequence Detection System (Applied Biosystems; Thermo Fisher Scientific, Inc.) The thermocycling conditions were as follows: Initial denaturation at 95˚C for 5 min; 36 cycles at 95˚C for 30 sec, 58˚C for 30 sec and 72˚C for 40 sec; and a final extension at 72˚C for 10 min. The following primer pairs were used for the qPCR: RPPH1 forward, 3'-CGAGCTGAGTGCGTC CTGTC-5' and reverse, 3'-TCGCTGGCCGTGAGTCTG T-5'; miR-326 forward, 3'-GGCGCCCAGAUAAUGCG-5' and reverse, 3'-CGTGCAGGGTCCGAGGTC-5'; WNT2B forward, 3'-CTGAAGAGCCCAAGCAAT-5' reverse, 3'-CTC CAAGGCCATCCAAC-5' and U6 forward, 3'-CTCGCTTCG GCAGCACA-5' and reverse, 3'-AACGCTTCACGAATT TGCGT-5'. U6 served as the internal control, and the relative expression of RPPH1, miR-326 and WNT2B was calculated using the $2^{-\Delta\Delta Cq}$ method (18).

Cell transfection. A549 and H1299 cells were plated at a density of $2x10^5$ cells/well in six-well plates with serum-free DMEM for transfections. RPPH1 short hairpin (sh) RNA (shRPPH1; 10 nM; 5'-UUGCCUUCAGUCGUGUGUAU CAG-3'; Shanghai Jima Biotechnology Co., Ltd.) and its negative control (sh-NC; 10 nM; 5'-AGUUCUGCGAACGUC GCACGU-3'; Shanghai Jima Biotechnology Co., Ltd.), were transfected into the cells. pcDNA3.1-RPPH1 overexpression vectors (GenePharma) and empty vectors (GenePharma) were also constructed to transfect cells. Further transfections were performed using a miR-326 mimic (10 nM; 5'-GCAGGGCAC GACUGAUCUUGG-3'), miR-326 inhibitor (10 nM; 5'-UCG CUCGGUCCYGAUCGGGAG-3') and their respective negative controls (miR-NC, 5'-GGAAGUCAUCCAAUGUGC AUU-3' and NC-inhibitor, 5'-UCCCUGGUUGCAGAUCGC GAA-3'). Co-transfection experiments were also carried out using combinations of RPPH1 vectors, WNT2B overexpression vector, miR-326 mimic and miR-326 inhibitor combinations. The miR-326 mimic, miR-326 inhibitor, miR-NC and WNT2B overexpression vectors were obtained from Shanghai Jima Biotechnology Co., Ltd. All transfections were carried out using Lipofectamine® 2000 (Invitrogen; Thermo Fisher Scientific, Inc.), following the manufacturer's instructions. Cells were incubated at 37˚C with 5% CO_2 for 8 h, and the medium was replaced with fresh DMEM containing 10% FBS. After 48-h incubation, cells were harvested for subsequent experimentation.

Transwell Matrigel assays. A549 and H1299 cells were harvested and re-suspended in serum-free DMEM medium at a density of $1x10^5$ cells/ml. A volume of 200 μl sample was added into Transwell chambers with 8-μm pores pre-coated with a layer of Matrigel. All Transwell chambers were then inserted into 24-well plates with 500 μl DMEM (10% FBS) added to the bottom of each well. The cells were incubated at 37˚C with 5% CO_2 for 48 h. The Transwell chambers were then removed and the membranes with adhered cells were collected. Cells on the upper surface of the membrane were gently scraped off using a cotton swab, whereas cells attached under the surface of the membrane were gently rinsed with PBS. Cells on the lower surface were fixed using 4% paraformaldehyde solution, then stained 0.1% crystal violet for 20 min at room temperature. The number of invading cells was counted under a light microscope (magnification, x200; Olympus Corporation).

Western blot analysis. Cells were collected and lysed on ice for 5 min using RIPA buffer (Beyotime Institute of Biotechnology). The cell lysate was then centrifuged for

10 min at 10,000 x g, 4˚C and the concentration of total protein in the supernatant was determined using a bicinchoninic acid kit (Thermo Fisher Scientific, Inc.). A total of 30 μg protein was resolved by SDS-PAGE on 10% gels (80 V for 30 min and 120 V for 60 min). Protein samples were transferred to a PVDF membrane at 110 V, which was then blocked with 5% skimmed milk for 2 h at room temperature. The membrane was subsequently incubated with the following primary antibodies (all 1:1,000; Abcam): Mouse anti-E-cadherin (1:1,000; cat. no. ab76055; Abcam), mouse anti-vimentin (1:1,000; cat. no. ab22651; Abcam), mouse anti-β-catenin (1:1,000; cat. no. ab231305; Abcam) and mouse anti-GAPDH (1:1,000; cat. no. ab8245; Abcam) for 12 h at 4˚C. After three washing steps with TBS-Tween-20 (TBS-T; 0.1% Tween-20), the membranes were incubated with secondary antibodies (Beijing Solarbio Science and Technology Co., Ltd.) for 1 h at room temperature. The membranes were washed three times in TBST, and the proteins bands were visualized using the Pierce ECL Western Blotting kit (Pierce; Thermo Fisher Scientific, Inc.). Protein expression was quantified using Image-Pro® Plus software (version 6.0; Media Cybernetics, Inc.). GAPDH was used as an internal control.

Cell Counting Kit-8 (CCK-8) assay. A549 and H1299 cells were seeded in 96-well plates at $1x10^4$ cells per well, in the presence or absence of 5 μg/ml cisplatin/cis-diamminedichloridoplatinum (CDDP; 100 μl; Sigma-Aldrich: Merck KGaA). Cell were incubated 37˚C, 5% CO_2 for 24, 48 and 72 h. A volume of 10 μl CCK-8 solution (Dojindo Molecular Technologies, Inc.) was added into each well, and the cells were incubated for 4 h at room temperature. After incubation, the optical density was measured in each well using a microplate reader at a wavelength of 450 nm. In this assay, optical density recording was proportional to cell viability and therefore indicative of cell resistance to CDDP.

Colony formation assay. A549 and H1299 cells were plated at a density of $1x10^3$ cells/dish in 90-mm cell culture dishes containing 5 ml complete DMEM complete + 10% FBS (with or without 5 μg/ml of CDDP). All dishes were placed in a sterile incubator at 37˚C with 5% CO_2 for 2 weeks. The medium was changed every two days. Cells were washed three times with PBS to remove residual cells then fixed in 4% formaldehyde for 10 min at room temperature. Crystal violet (0.1%) was then used to stain cells for 10 min at room temperature. Colonies were counted under a light microscope. Groups of >50 cells were considered a clone.

Luciferase reporter gene assay. StarBase 2.0 (http://starbase.sysu.edu.cn) was used to predict the potential miRNAs that can bind to RPPH1, and TargetScan 7.2 (http://www.targetscan.org) was used to predict the potential downstream target of miR-326. Wild-type RPPH1, mutant RPPH1, wild-type WNT2B and mutant WNT2B constructs were designed and purchased from Shanghai GenePharma Co., Ltd. All four constructs were cloned into the pmirGLO reporter vectors. A549 cells were seeded into six-well plates at a density of $2x10^5$ cells/well and co-transfected with the miR-NC, miR-326 mimic, NC-inhibitor and miR-326 inhibitor group, as well as the pmirGLO reporter vectors using Lipofectamine® 2000 (Invitrogen; Thermo Fisher Scientific, Inc.). After 48-h incubation at 37˚C with 5% CO_2, cells were collected and lysed. To obtain the supernatant, solutions were centrifuged for 10 min at 10,000 x g and 4˚C. The luciferase activity of cells was detected using the Dual-Luciferase Reporter Assay System (Promega Corporation). *Renilla* luciferase activity was used as internal reference.

Statistical analysis. All experiments were repeated at least three times. Statistical analysis was conducted using SPSS 19.0 (IBM Corp.). Kaplan-Meier curves and the log-rank test were used to compare differences in patient survival times. Cut-off values were determined using median of expression. Differential gene expression among tumor stages was evaluated by one-way ANOVA, and violin plots were generated using the 'vioplot' R package (http://CRAN.R-project.org/package=vioplot). Comparisons between two groups were carried out using Student's t-test. Multigroup comparisons were performed using one-way ANOVA, followed by Tukey's post hoc test. $P<0.05$ was considered to indicate a statistically significant difference.

Results

High RPPH1 expression levels is associated with poor prognosis in patients with NSCLC. RPPH1 expression levels were significantly higher in four NSCLC cell lines (H358, A549, H1299 and H1650), compared with the BEAS-2B normal lung epithelial cell line (Fig. 1A). The association between RPPH1 expression levels and the prognosis of patients with NSCLC was also analyzed in data obtained from TCGA. RPPH1 expression was significantly increased in NSCLC tumor tissues compared with normal tissues (Fig. 1B). Furthermore, patients with low RPPH1 expression levels exhibited significantly higher 80-month overall survival compared with patients with high RPPH1 levels (Fig. 1C). The RPPH1 expression levels in patients with stage-IV NSCLC was also markedly higher compared with patients with stage I, II and III (Fig. 1D). Therefore, high RPPH1 expression levels in patients with NSCLC were associated with poor prognosis.

RPPH1 knockdown inhibits NSCLC cell invasion, epithelial-mesenchymal transition (EMT) and drug resistance. Since A549 and H1299 cell lines presented the higher expression of RPPH1, A549 and H1299 were used in the following experiments and were transfected with shRPPH1 or shNC. RPPH1 expression significantly declined in A549 and HI1299 cells transfected with shRPPH1 compared with the shNC group (Fig. 2A). In addition, a significant reduction in the number of invading cells was also observed in the shRPPH1 group compared with the shNC group (Fig. 2B). Higher E-cadherin and lower vimentin protein expression levels were detectable in A549 and H1299 cells following transfection with shRPPH, compared with shNC (Fig. 2C).

The expression of RPPH1 was significantly upregulated in A549 and H1299 cells transfected with RPPH1 overexpression plasmid compared with the empty vector NC (Fig. 2D). Furthermore, cell viability and colony numbers were significantly reduced in A549 and H1299 cells in response to CDDP treatment, compared with untreated cells. However, RRHP1

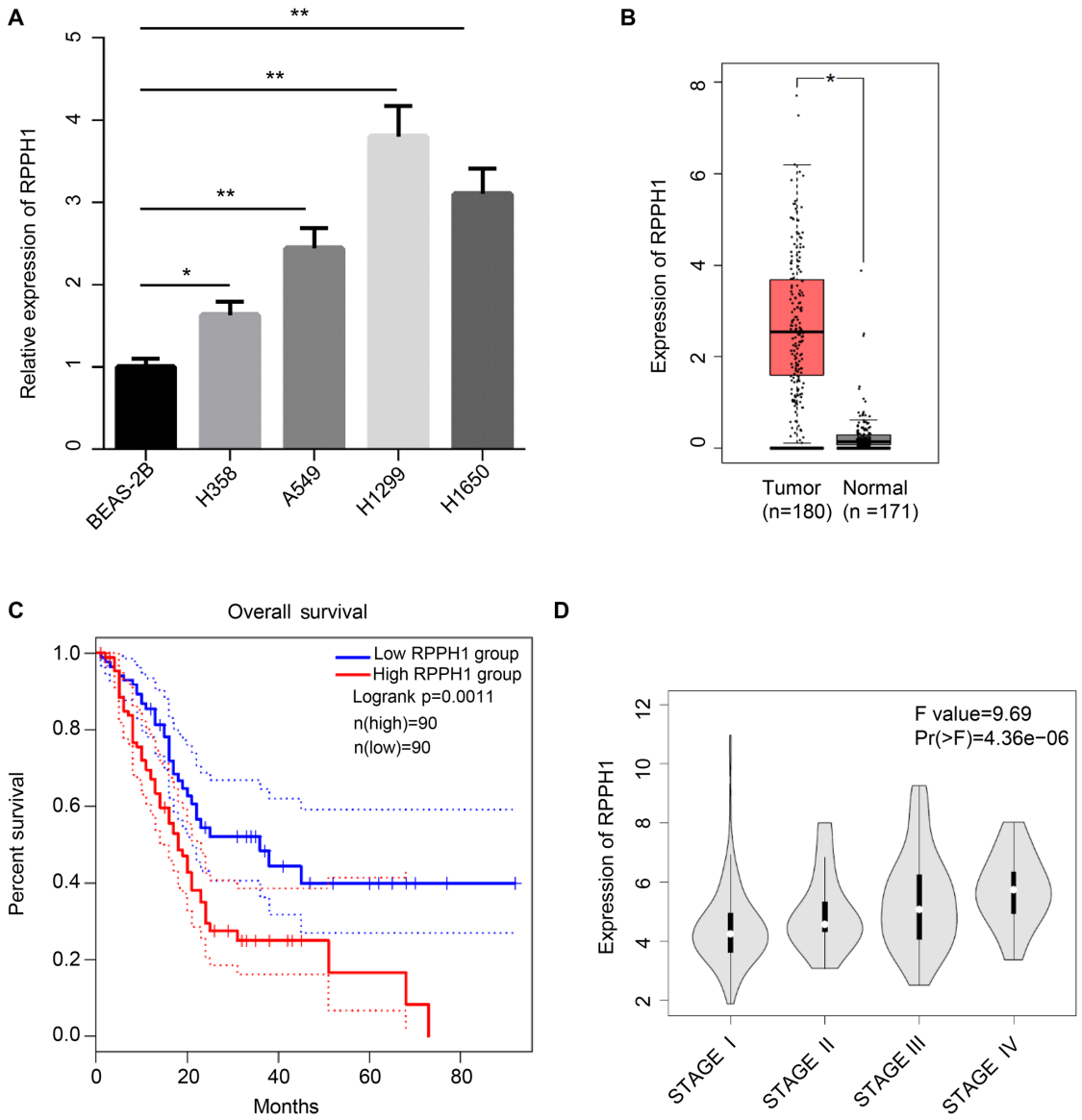

Figure 1. RPPH1 overexpression in NSCLC is associated with poor prognosis. (A) RPPH1 expression levels in human cell lines were evaluated using reverse transcription-quantitative PCR. (B) RPPH1 expression levels in TCGA datasets from NSCLC tumor tissue and normal tissue. (C) Analysis of 80-month overall survival in TCGA datasets from patients with NSCLC. (D) Relationship between RPPH1 expression levels and the NSCLC clinical stages in TCGA datasets. *P<0.05 and **P<0.01. NSCLC, non-small cell lung carcinoma; RPPH1, ribonuclease P RNA component H1; TCGA, The Cancer Genome Atlas.

overexpression resulted in a significant increase in cell viability and higher colony numbers in response to CDDP compared with CDDP-treated, NC-transfected cells (Fig. 2E-G). Collectively, these observations indicated that RPPH1 could increase the resistance of A549 and H1299 to CDDP treatment.

miR-326 inhibitor partially rescues the cell phenotype caused by RPPH1 knockdown. According to Starbase 2.0, RPPH1 contains a potential binding site for miR-326 in its 3'-untranslated (3'-UTR) region (Fig. 3A). Transfection with miR-326 mimic significantly increased the expression of miR-326, whereas the miR-326 inhibitor significantly decreased miR-326 expression, compared with their respective controls (Fig. 3B). To validate the potential interaction between RPPH1 and miR-326, dual luciferase reporter assays were performed. Compared with miR-NC, miR-326 mimic significantly reduced the luciferase activity of cells transfected with wild-type RPPH1 luciferase construct, but not with the mutant. Similarly, the miR-326 inhibitor significantly increased the luciferase activity of cells transfected with wild-type, but not mutant, RPPH1 luciferase constructs (Fig. 3C). Moreover, compared with shNC transfection shRPPH1-transfected A549 cells demonstrated significantly higher miR-326 expression levels, significantly lower numbers of invasive cells, higher E-cadherin expression levels and reduced vimentin protein expression levels. However, co-transfection with shRPPH1 and miR-326 inhibitor resulted in significantly lower miR-326 expression levels, significantly higher invasive cell frequencies, reduced E-cadherin levels and increased vimentin protein expression, compared with shRPPH1 alone (Fig. 3D-F).

The resistance of A549 cells to CDDP was then evaluated using CCK-8 and colony formation assays. A549 cells transfected with the RPPH1 overexpression vector displayed significantly higher viability and greater colony numbers,

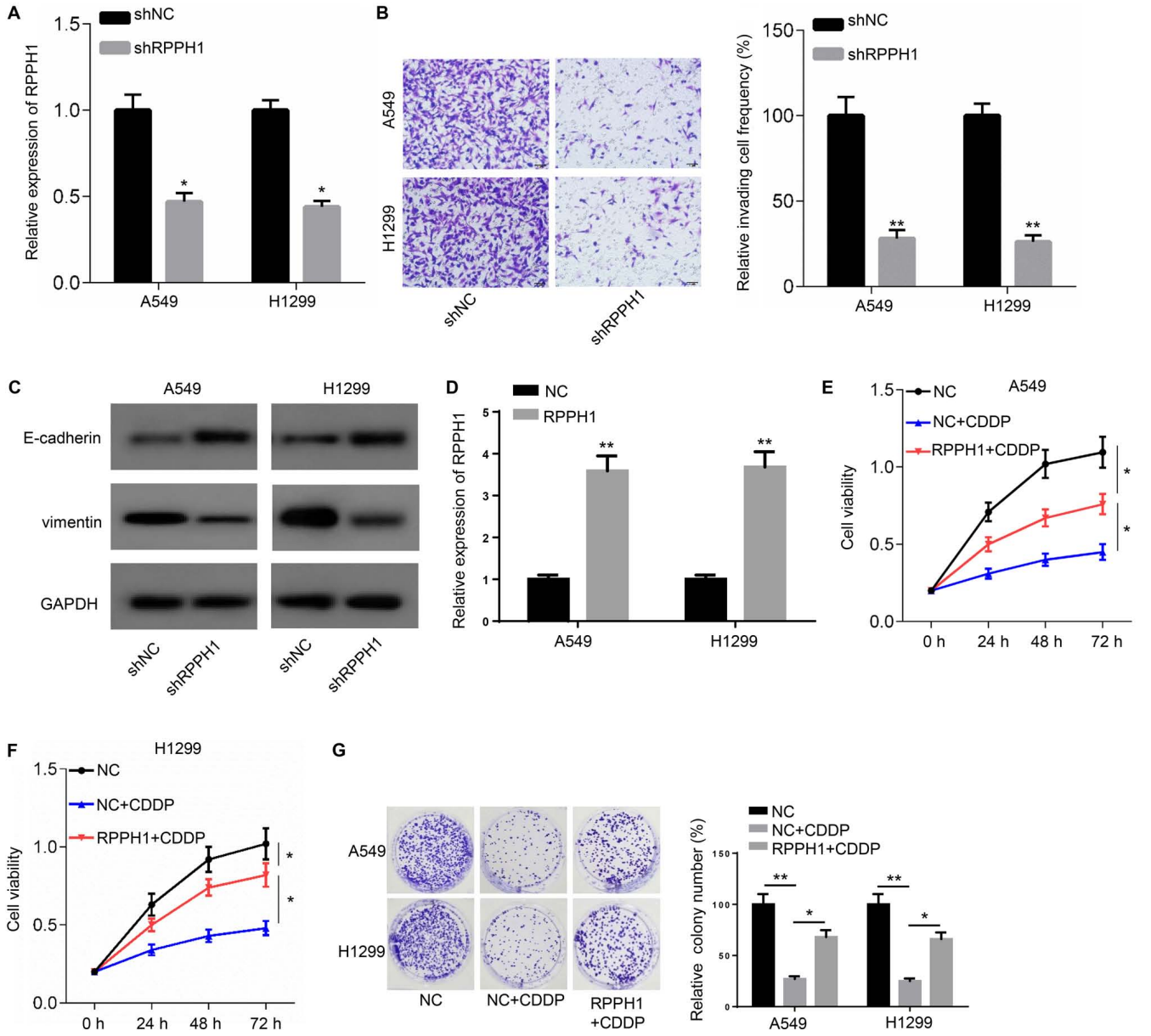

Figure 2. RPPH1 knockdown inhibits NSCLC cell invasion, epithelial-mesenchymal transition and drug resistance. (A) RPPH1 mRNA levels in A549 and H1299 cells transfected with shRRPH1. (B) A549 and H1299 cell invasion was assessed using Transwell Matrigel assays (magnification, x100; scale bar, 50 μm). (C) E-cadherin and vimentin protein levels in A549 and H1299 cells. (D) RPPH1 mRNA levels in A549 and H1299 cells transfected with RPPH1 overexpression vector. Resistance of (E) A549 and (F) H1299 cells to CDDP was determined using Cell Counting Kit-8 assays. (G) Resistance of A549 and H1299 cells to CDDP was evaluated using colony formation assays. *P<0.05 and **P<0.01. NSCLC, non-small cell lung carcinoma; RPPH1, ribonuclease P RNA component H1; sh, short hairpin; CDDP, cisplatin/cis-diamminedichloroplatinum; NC, negative control.

compared with the empty vector NC (Fig. 3G and H). However, cell viability and colony numbers were significantly reduced in cells transfected with RPPH1 + miR-326 mimic, compared with RRPH1 alone. Altogether, these results suggested that the role of RPPH1 may be mediated by miR-326.

miR-326 directly inhibits the Wnt signaling pathway. TargetScan 7.2 predicted that the miR-326 sequence contained a binding site in the 3'-UTR region of WNT2B (Fig. 4A). In a dual luciferase reporter assay, the luciferase activity of wild-type WNT2B, but not the mutant construct, was significantly decreased following co-transfection with miR-326 mimic, compared with miR-NC. By contrast, miR-326 inhibitor transfection significantly increased the wild-type WNT2B luciferase activity, but not that of the mutant WNT2B (Fig. 4B).

WNT2B expression was significantly increased in A549 cells transfected with miR-326 mimic compared with miR-NC. Conversely, transfection with miR-326 inhibitor resulted in significantly higher WNT2B expression compared with the NC inhibitor group (Fig. 4C). These results indicated that WNT2B was directly inhibited by miR-326.

WNT2B partially rescues the cell phenotype induced by miR-326 overexpression. The expression of WNT2B was significantly upregulated in A549 cells transfected WNT2B overexpression plasmid compared with the NC group (Fig. 5A). Relative to the miR-NC group, reduced WNT2B expression levels and

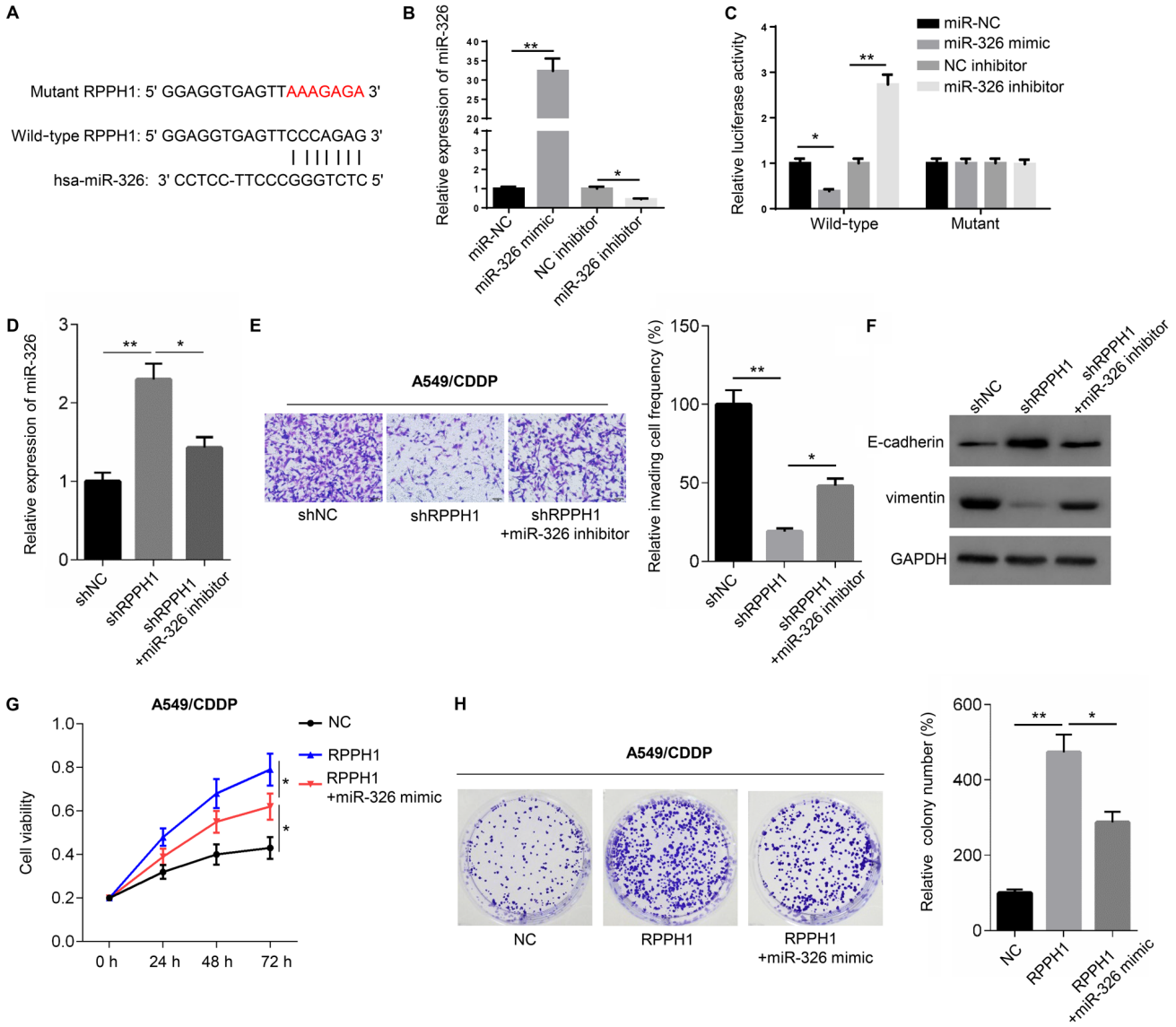

Figure 3. miR-326 silencing partially reverses the effects of RPPH1 knockdown. (A) Starbase prediction of the binding site between RPPH1 and miR-326. (B) miR-326 expression in A549 cells transfected with miR-326 mimic or inhibitor. (C) RPPH1 luciferase reporter assays were carried out in A549 cells transfected with miR-326 mimic or inhibitor. (D) miR-326 levels, (E) Invasion potential (magnification, x100; scale bar, 50 μm) and (F) E-cadherin and vimentin protein levels in A549 cells transfected with shRPPH1 alone or with miR-326 inhibitor. (G) Cell Counting Kit-8 and (H) colony formation assays were performed to evaluate CDDP resistance of A549 cells transfected with RPPH1 overexpression vector alone or with miR mimic. *P<0.05, **P<0.01. miR, microRNA; RPPH1, ribonuclease P RNA component H1; CDDP, cisplatin/cis-diamminedichloroplatinum; sh, short hairpin; NC, negative control.

invasive cell frequencies were observed in A549 cells transfected with miR-326 mimic. Moreover, E-cadherin expression was increased, while vimentin levels were reduced in miR-326 mimic-transfected cells compared with the miR-NC groups. However, co-transfection with miR-326 mimic and WNT2B overexpression vector resulted in higher WNT2B expression levels, compared with mimic transfection alone. miR-326 mimic and WNT2B overexpression also resulted in a significant increase in the frequency of invading cells, a reduction in E-cadherin protein expression and an increase in vimentin protein expression compared with the miR-326 mimic groups (Fig. 5B-D). In addition, lower β-catenin protein expression was observed in miR-326 mimic-transfected A549 cells compared with miR-NC. However, the expression of β-catenin increased in cells co-transfected with miR-326 mimic and WNT2B overexpression vector compared with cells transfected with the mimic alone (Fig. 5E)

The aforementioned co-transfection experiments were also carried out in the presence or absence of 5 μg/ml CDDP in order to evaluate drug resistance in each of the groups. Cell viability and colony numbers were significantly reduced in miR-326 mimic-transfected cells, compared with the miR-NC group. However, co-transfection with the miR-326 mimic and WNT2B overexpression vector significantly increased cell viability and colony numbers, compared with transfection with the miR-326 mimic alone (Fig. 5F and G). Thus, WNT2B partially rescued the cell phenotype induced by miR-326 overexpression.

Discussion

The present study demonstrated that RPPH1 was upregulated in NSCLC tissues. Moreover, high RPPH1 expression was

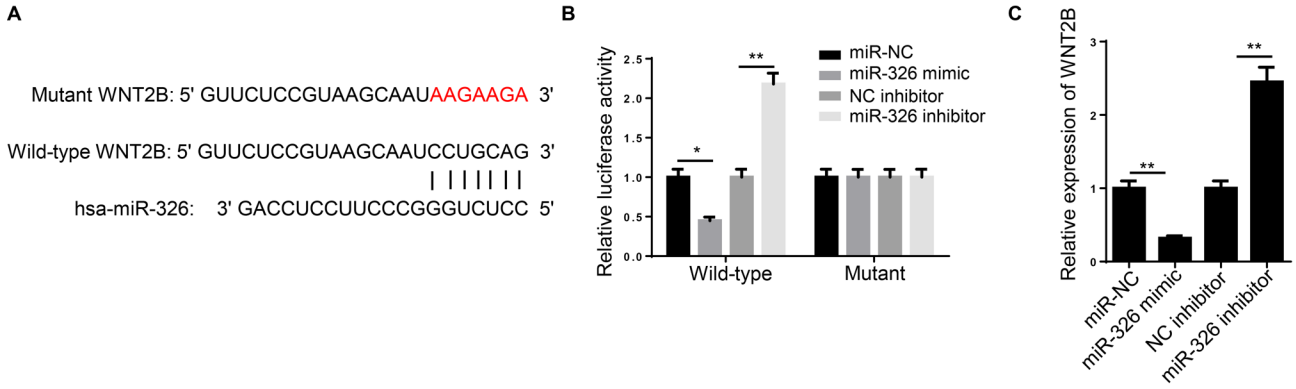

Figure 4. miR-326 directly inhibits the Wnt signaling pathway. (A) TargetScan prediction of the miR-326 binding site in the WNT2B 3'-untranslated region. (B) WNT2B luciferase reporter assays were carried out in A549 cells transfected with miR-326 mimic or inhibitor. (C) WNT2B expression levels in A549 cells transfected with miR-326 mimic or inhibitor. *P<0.05 and **P<0.01. miR, microRNA; WNT2B, Wnt family member 2B; NC, negative control.

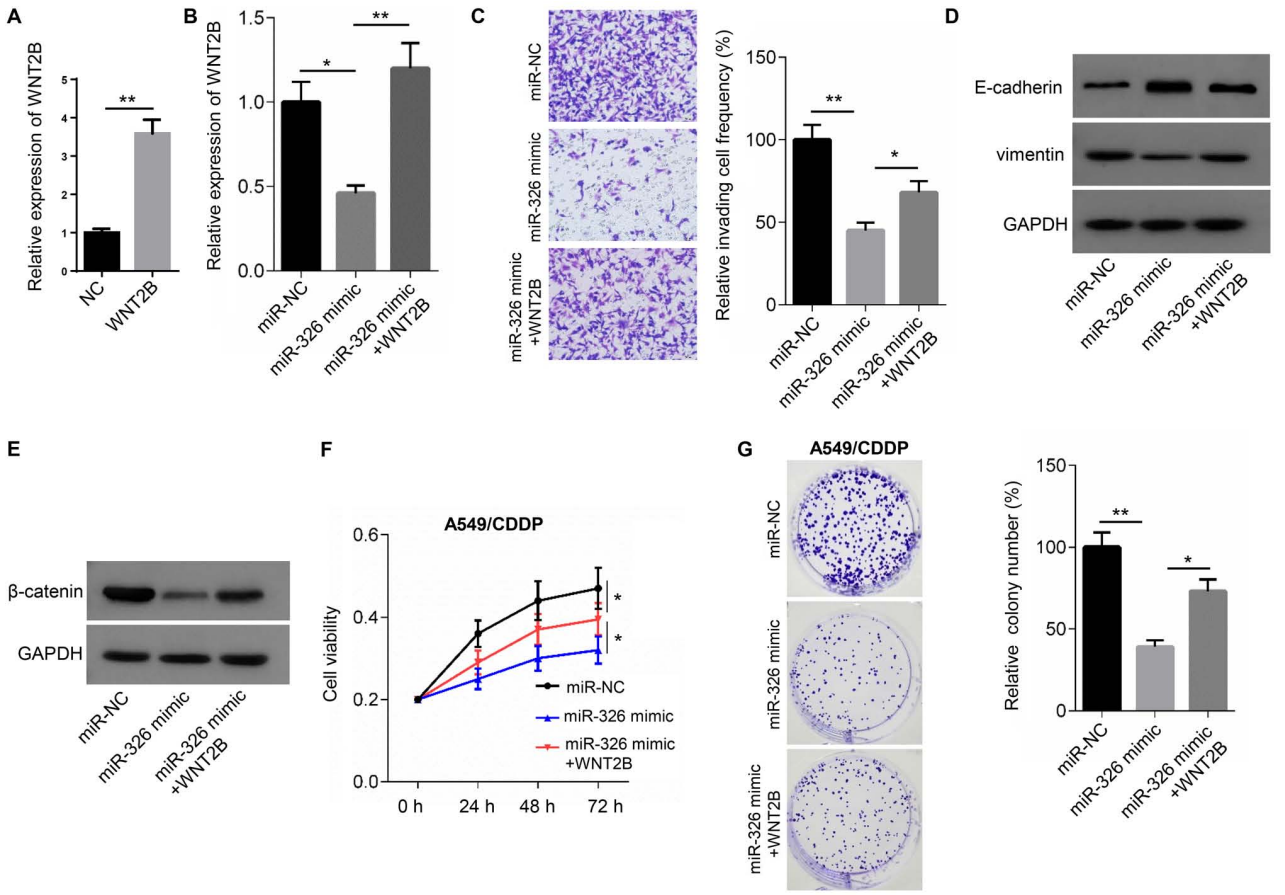

Figure 5. WNT2B partially rescues the cell phenotype induced by overexpression of miR-326. (A) WNT2B expression in A549 cells transfected with WNT2B overexpression vector or NC. (B) WNT2B expression in A549 cells transfected with miR-326 alone or with WNT2B overexpression vector. (C) Invasion potential (magnification, x100; scale bar, 50 μm) and (D) E-cadherin and vimentin protein expression levels in A549 cells transfected with miR-326 alone or with WNT2B overexpression vector. (E) β-catenin protein expression levels in A549 cells transfected with miR-326 alone or with WNT2B overexpression vector. (F) Cell Counting Kit-8 and (G) colony formation assays were performed to evaluate the CDDP resistance of A549 cells transfected with miR-326 alone or with WNT2B overexpression vector. *P<0.05, **P<0.01. miR, microRNA; WNT2B, Wnt family member 2B; NC, negative control; CDDP, cisplatin/cis-diamminedichloroplatinum.

associated with poor prognosis, including low 80-month overall survival and advanced clinical stages. *In vitro* experiments further indicated that RPPH1 could promote NSCLC progression via regulation of miR-326 and WNT2B.

NSCLC is a major malignant tumor type and a leading cause of cancer-related deaths worldwide, accounting for 85% of all lung cancer cases (19). At the time of diagnosis, most patients with NSCLC are already at a locally advanced stage of the disease or have distantly metastatic tumors (20). The 5-year survival rate is particularly low in patients with advanced NSCLC, reaching only 4% (21). NSCLC pathogenesis is not fully understood, which may account for the lack of

adequate therapeutic strategies available to patients with this disease.

In recent years, lncRNAs have been considered to be potential target for the treatment of NSCLC due to their regulatory role in the development of this cancer type (22). LncRNAs are a class of RNA molecules >200 nucleotides in length (23). Despite their lack of protein-coding function, lncRNAs have been demonstrated to regulate gene expression (24). LncRNAs participate in a variety of cellular biological processes, including chromatin modification, epigenetic regulation, cell cycle regulation, nucleoplasm transport, transcription, translation and cell differentiation (25,26). Therefore, dysregulation of lncRNA function could lead to the onset and progression of diseases, including tumors.

RPPH1 is an RNA subunit of RNase P, which is reported to be abnormally overexpressed in the neocortex of patients with seizures and in tumor tissues of patients with gastric or breast cancer (10,27,28). However, to the best of the authors' knowledge, the relationship between RPPH1 and NSCLC has not been examined to date. In the present study, RPPH1 was demonstrated to promote NSCLC progression and to enhance the resistance of NSCLC cells to CDDP by regulating the miR-326/WNT2B axis. Mechanistically, RPPH1 might enhance NSCLC progression by competitively binding to miR-326, thereby inhibiting the binding of miR-326 to its target gene, WNT2B. Consistent with this hypothesis, previous studies have suggested that miR-326 expression is decreased in NSCLC primary tumor tissue and NSCLC cells, and that miR-326 inhibits NSCLC cell migration and invasion by suppressing the expression of the G1/S-specific cyclin-D1 oncogene (29). The present findings suggested that RPPH1 silencing reduced the invasion potential and EMT in NSCLC cell lines. Moreover, downregulation of miR-326 partially rescued this phenotype.

In several types of human malignancies, including lung cancer, resistance to CDDP is a major obstacle to successful therapy (30). The present study indicated that RPPH1 overexpression could increase the CDDP resistance of NSCLC cells. Moreover, miR-326 overexpression reversed the CDDP resistance conferred by RPPH1 upregulation. Similarly, Li *et al* (31) demonstrated that miR-326 was downregulated in CDDP-resistant A549 cells compared with wild-type A549 cells. Furthermore, patients with lung adenocarcinoma receiving CDDP chemotherapy displayed reduced miR-326 levels in their tumor tissues (31). Consistent with these previous findings, miR-326 acted as a tumor suppressor in NSCLC tissue in the present study and could inhibit CDDP resistance induced by RPPH1 overexpression.

WNT2B is a paralogue of WNT2 and is one of the key molecules in the Wnt signaling pathway (32). WNT2B promotes the progression of head and neck squamous cell carcinoma, malignant pleural mesothelioma, ovarian cancer and pancreatic cancer, and enhances chemotherapy resistance and metastasis, leading to poor prognosis (33-36). In nasopharyngeal carcinoma cells, WNT2B expression is directly upregulated by decreased miR-324-3p expression levels, which in turn enhances migration, invasion and EMT (37). Furthermore, Wang *et al* (16) suggested that abnormally elevated WNT2B expression levels in NSCLC cells were the result of miR-577 downregulation. High expression of WNT2B is associated with a malignant phenotype in NSCLC cells, including enhanced cell viability, migration and invasion (16). One possible underlying mechanism may be that reduced miR-577 expression promotes the Wnt/β-catenin pathway by regulating WNT2B expression. The aforementioned previous studies emphasize the oncogenic role of WNT2B in human malignant tumor types. Similarly, the present study also demonstrated that WNT2B expression was increased in NSCLC cells through the downregulation of miR-326 and that WNT2B could promote NSCLC cell invasion, EMT and resistance to CDDP.

In conclusion, RPPH1 acted an oncogene in NSCLC, which enhanced NSCLC progression and resistance to CDDP through the miR-326/WNT2B axis. The present article provides a theoretical framework the development of therapeutic strategies for NSCLC, with RPPH1 as a novel molecular target for NSCLC treatment.

Acknowledgements

Not applicable.

Funding

No funding was received.

Availability of data and materials

The datasets used and/or analyzed during the present study are available from the corresponding author upon reasonable request.

Authors' contributions

YW and XW contributed to the conception and design of the study. KC, WL, XW and YW performed the experiments. YW and KC analyzed the data. YW and XW wrote the manuscript. All authors read and approved the final manuscript.

Ethics approval and consent to participate

Not applicable.

Patient consent for publication

Not applicable.

Competing interests

The authors declare that they have no competing interests.

References

1. Brahmer JR, Govindan R, Anders RA, Antonia SJ, Sagorsky S, Davies MJ, Dubinett SM, Ferris A, Gandhi L, Garon EB, *et al*: The Society for Immunotherapy of Cancer consensus statement on immunotherapy for the treatment of non-small cell lung cancer (NSCLC). J Immunother Cancer 6: 75, 2018.
2. Lei Z, Shi H, Li W, Yu D, Shen F, Yu X, Lu D, Sun C and Liao K: MiR-185 inhibits non-small cell lung cancer cell proliferation and invasion through targeting of SOX9 and regulation of Wnt signaling. Mol Med Rep 17: 1742-1752, 2018.

3. Tanaka F and Yoneda K: Adjuvant therapy following surgery in non-small cell lung cancer (NSCLC). Surg Today 46: 25-37, 2016.
4. Sotgia F and Lisanti MP: Mitochondrial markers predict survival and progression in non-small cell lung cancer (NSCLC) patients: Use as companion diagnostics. Oncotarget 8: 68095-68107, 2017.
5. Yin D, Lu X, Su J, He X, De W, Yang J, Li W, Han L and Zhang E: Long noncoding RNA AFAP1-AS1 predicts a poor prognosis and regulates non-small cell lung cancer cell proliferation by epigenetically repressing p21 expression. Mol Cancer 17: 92, 2018.
6. Guo X, Wei Y, Wang Z, Liu W, Yang Y, Yu X and He J: LncRNA LINC00163 upregulation suppresses lung cancer development though transcriptionally increasing TCF21 expression. Am J Cancer Res 8: 2494-2506, 2018.
7. Pei W, Dong C, Hongbing M and Yong L: Long non-coding RNA MEG3 regulates proliferation and apoptosis in non-small cell lung cancer via the miR-205-5p/LRP1 pathway. Rsc Adv 7: 49710-49719, 2017.
8. Cai Y, Sun Z, Jia H, Luo H, Ye X, Wu Q, Xiong Y, Zhang W and Wan J: Rpph1upregulates CDC42 expression and promotes hippocampal neuron dendritic spine formation by competing with miR-330-5p. Front Mol Neurosci 10: 27, 2017.
9. Zhang, P., Sun, Y., Peng, R. et al. Long non-coding RNA Rpph1 promotes inflammation and proliferation of mesangial cells in diabetic nephropathy via an interaction with Gal-3. Cell Death Dis 10: 526. 2019.
10. Liang ZX, Liu HS, Wang FW, Xiong L,Zhou C, Hu T, He XW, Wu XJ, Xie D,Wu XR and Lan P: LncRNA RPPH1 promotes colorectal cancer metastasis by interacting with TUBB3 and by promoting exosomes-mediated macrophage M2 polarization. Cell Death Dis 10: 829, 2019.
11. Lei B, He A, Chen Y, Cao X, Zhang P, Liu J, Ma X, Qian L and Zhang W: Long non-coding RNA RPPH1 promotes the proliferation, invasion and migration of human acute myeloid leukemia cells through down-regulating miR-330-5p expression. EXCLI J 18: 824-837, 2019.
12. Jiang H, Liang M, Jiang Y, Zhang T, Mo K, Su S, Wang A, Zhu Y, Huang G and Zhou R: The lncRNA TDRG1 promotes cell proliferation, migration and invasion by targeting miR-326 to regulate MAPK1 expression in cervical cancer. Cancer Cell Int 19: 152, 2019.
13. Wang R, Chen X, Xu T, Xia R, Han L, Chen W, De W and Shu Y: MiR-326 regulates cell proliferation and migration in lung cancer by targeting phox2a and is regulated by HOTAIR. Am J Cancer Res 6: 173-186, 2016.
14. Ghaemi Z, Soltani BM and Mowla SJ: MicroRNA-326 functions as a tumor suppressor in breast cancer by targeting ErbB/PI3K signaling pathway. Front Oncol 9: 653, 2019.
15. Liu W, Zhang B, Xu N, Wang MJ and Liu Q: MiR-326 regulates EMT and metastasis of endometrial cancer through targeting TWIST1. Eur Rev Med Pharmacol Sci 21: 3787-3793, 2017.
16. Wang B, Sun L, Li J and Jiang R: MiR-577 suppresses cell proliferation and epithelial-mesenchymal transition by regulating the WNT2B mediated Wnt/β-catenin pathway in non-small cell lung cancer. Mol Med Rep 18: 2753-2761, 2018.
17. Detterbeck FC, Boffa DJ, Kim AW and Tanoue LT: The eighth edition lung cancer stage classification. Chest 151: 193-203, 2017.
18. Livak KJ and Schmittgen TD: Analysis of relative gene expression data using real-time quantitative PCR and the 2(-Delta Delta C(T)) method. Methods 25: 402-408, 2001.
19. Hai J, Zhu CQ, Wang T, Organ SL, Shepherd FA and Tsao MS: TRIM14 is a putative tumor suppressor and regulator of innate immune response in non-small cell lung cancer. Sci Rep 7: 39692, 2017.
20. Stinchcombe TE and Socinski MA: Current treatments for advanced stage non-small cell lung cancer. Proc Am Thorac Soc 6: 233-241, 2009.
21. Siegel RL, Miller KD and Jemal A: Cancer statistics, 2017. CA Cancer J Clin 67: 7-30, 2017.
22. Wang L, Ma L, Xu F, Zhai W, Dong S, Yin L, Liu J and Yu Z: Role of long non-coding RNA in drug resistance in non-small cell lung cancer. Thorac Cancer 9: 761-768, 2018.
23. Schmitt AM and Chang HY: Long Noncoding RNAs in cancer pathways. Cancer Cell 29: 452-463, 2016.
24. Noh JH, Kim KM, McClusky WG, Abdelmohsen K and Gorospe M: Cytoplasmic functions of long noncoding RNAs. Wiley Interdiscip Rev RNA 9: e1471, 2018.
25. Chen QN, Wei CC, Wang ZX and Sun M: Long non-coding RNAs in anti-cancer drug resistance. Oncotarget 8: 1925-1936, 2017.
26. Jiang C, Li X, Zhao H and Liu H: Long non-coding RNAs: Potential new biomarkers for predicting tumor invasion and metastasis. Mol Cancer 15: 62, 2016.
27. Xia T, Liao Q, Jiang X, Shao Y, Xiao B, Xi Y and Guo J: Long noncoding RNA associated-competing endogenous RNAs in gastric cancer. Sci Rep 4: 6088, 2014.
28. Leonard L, Dachet F, Cai J, Bagla S, Balan K, Jia H and Loeb JA: Activity-dependent human brain coding/noncoding gene regulatory networks. Genetics 192: 1133-1148, 2012.
29. Sun C, Huang C, Li S, Yang C, Xi Y, Wang L, Zhang F, Fu Y and Li D: Hsa-miR-326 targets CCND1 and inhibits non-small cell lung cancer development. Oncotarget 7: 8341-8359, 2016.
30. Sun Y, Zheng S, Torossian A, Speirs CK, Schleicher S, Giacalone NJ, Carbone DP, Zhao Z and Lu B: Role of insulin-like growth factor-1 signaling pathway in cisplatin-resistant lung cancer cells. Int J Radiat Oncol Biol Phys 82: e563-e572, 2012.
31. Li J, Li S, Chen Z, Wang J, Chen Y, Xu Z, Jin M and Yu W: MiR-326 reverses chemoresistance in human lung adenocarcinoma cells by targeting specificity protein 1. Tumour Biol 37: 13287-13294, 2016.
32. Katoh M: Differential regulation of WNT2 and WNT2B expression in human cancer. Int J Mol Med 8: 657-660, 2001.
33. Li SJ, Yang XN and Qian HY: Antitumor effects of WNT2B silencing in GLUT1 overexpressing cisplatin resistant head and neck squamous cell carcinoma. Am J Cancer Res 5: 300-308, 2014.
34. Kobayashi M, Huang CL, Sonobe M, Kikuchi R, Ishikawa M, Kitamura J, Miyahara R, Menju T, Iwakiri S, Itoi K, *et al*: Intratumoral Wnt2B expression affects tumor proliferation and survival in malignant pleural mesothelioma patients. Exp Ther Med 3: 952-958, 2012.
35. Wang H, Fan L, Xia X, Rao Y, Ma Q, Yang J, Lu Y, Wang C, Ma D and Huang X: Silencing Wnt2B by siRNA interference inhibits metastasis and enhances chemotherapy sensitivity in ovarian cancer. Int J Gynecol Cancer 22: 755-761, 2012.
36. Jiang H, Li F, He C, Wang X, Li Q and Gao H: Expression of Gli1 and Wnt2B correlates with progression and clinical outcome of pancreatic cancer. Int J Clin Exp Pathol 7: 4531-4538, 2014.
37. Liu C, Li G, Yang N, Su Z, Zhang S, Deng T, Ren S, Lu S, Tian Y, Liu Y and Qiu Y: MiR-324-3p suppresses migration and invasion by targeting WNT2B in nasopharyngeal carcinoma. Cancer Cell Int 17: 2, 2017.